Chinese Journal of Natural Medicines

Atramacronins AP, eudesmane-type sesquiterpenoid dimers from *Atractylodes macrocephala* with anti-hepatocellular carcinoma activities

Ganggang Zhou, Xinru Li, Jiajia Liu, Jiqiong Wang, Zhaoyue Dong, Ammara Khalid, Yinda Qiu, Zhihua Liao, Guowei Wang, Hui Liu, Qingwen Zhang, Min Chen, Fancheng Meng

Citation: Ganggang Zhou, Xinru Li, Jiajia Liu, Jiqiong Wang, Zhaoyue Dong, Ammara Khalid, Yinda Qiu, Zhihua Liao, Guowei Wang, Hui Liu, Qingwen Zhang, Min Chen, Fancheng Meng, Atramacronins AP, eudesmane-type sesquiterpenoid dimers from *Atractylodes macrocephala* with anti-hepatocellular carcinoma activities, Chinese Journal of Natural Medicines, 2026, 24(1), 119-128. doi: 10.1016/S1875-5364(26)61082-5.

View online: https://doi.org/10.1016/S1875-5364(26)61082-5

Chinese Journal of Natural Medicines 24 (2026) 119-128

Contents lists available at ScienceDirect

Chinese Journal of Natural Medicines

journal homepage: www.cjnmcpu.com/

Original article

Atramacronins A–P, eudesmane-type sesquiterpenoid dimers from *Atractylodes macrocephala* with anti-hepatocellular carcinoma activities

Ganggang Zhou[a,b], Xinru Li[a], Jiajia Liu[a], Jiqiong Wang[a], Zhaoyue Dong[a], Ammara Khalid[a], Yinda Qiu[a], Zhihua Liao[c], Guowei Wang[a], Hui Liu[d], Qingwen Zhang[e], Min Chen[a,b,*], Fancheng Meng[a,b,*]

[a] *Chongqing Key Laboratory of New Drug Screening from Traditional Chinese Medicine, Integrative Science Center of Germplasm Creation in Western China (Chongqing) Science City & Southwest University, SWU-TAAHC Medicinal Plant Joint R&D Centre, College of Pharmaceutical Sciences, Southwest University, Chongqing 400715, China*

[b] *Key Laboratory of Luminescence Analysis and Molecular Sensing, Ministry of Education, College of Pharmaceutical Sciences, Southwest University, Chongqing 400715, China*

[c] *Integrative Science Center of Germplasm Creation in Western China (Chongqing) Science City & Southwest University, School of Life Sciences, Southwest University, Chongqing 400715, China*

[d] *School of Medicine, Foshan University, Foshan 528225, China*

[e] *State Key Laboratory of Quality Research in Chinese Medicine, Institute of Chinese Medical Sciences, University of Macau, Macao SAR, China*

ARTICLE INFO

Article history:
Received 2 February 2025
Revised 18 May 2025
Accepted 3 July 2025
Available online 20 January 2026

Keywords:
Atractylodes macrocephala
Sesquiterpenoid
Cytotoxic activity
Hepatocellular carcinoma

ABSTRACT

Atractylodes macrocephala Koidz. (*A. macrocephala*) is a medicinal and edible plant species belonging to the Compositae family. Its rhizome serves both therapeutic and nutritional purposes in China. This investigation led to the isolation of thirteen novel rearranged 9(8→7)-*abeo*-eudesmane-type sesquiterpenoid dimers (SDs), atramacronins A–M (**1**–**13**), three eudesmane-type SDs, atramacronins N–P (**14**–**16**), and two previously identified meroterpenoids, atrachinenin G (**17**) and atrachinenin I (**18**), from *Atractylodes macrocephala*. Structure elucidation was accomplished through comprehensive spectroscopic analysis and single-crystal X-ray diffraction. Compounds **1**, **4**–**7**, **9**, and **10** exhibited notable cytotoxicity against Hep3B, HepG2, and Huh7 cell lines, with half maximal inhibitory concentration (IC_{50}) values ranging from 3.71 to 13.99 μmol·L^{-1}.

1. Introduction

Atractylodes macrocephala Koidz. (*A. macrocephala*, Chinese name: Baizhu), a member of the Compositae family, serves both medicinal and edible purposes in China. Its rhizome represents one of the most widely used traditional Chinese medicines, particularly for treating spleen deficiency syndrome [1] and hepatocellular carcinoma (HCC). Several formulations containing Atractylodis Macrocephalae Rhizoma (Baizhu), such as Guipi Decoction, Qingfu-Jindan, Xiaoyao San, and Ganfule, have been recommended as adjuvant therapies for HCC during perioperative care, rehabilitation, and palliative stages. This recommendation is outlined in the 2022 edition of the *Diagnosis and Treatment Guidelines for Primary Liver Cancer* issued by the Chinese Society of Clinical Oncology. Baizhu also serves as a crucial component in formulas such as Yupingfeng San [2] and Fuzheng Jiedu Xiaoji Formula [3], which demonstrate notable therapeutic effects on HCC.

Sesquiterpenoids are recognized as the primary active components of *A. macrocephala* [4]. Atractylenolides derived from *A. macrocephala* demonstrate anti-tumor effects across various cancer types [5]. Notably, sesquiterpenoid dimers (SDs) have garnered significant attention in recent years due to their unique structural characteristics and substantial pharmacological activities [6-10]. While two high-content SDs in *A. macrocephala*, biatractylenolide and biepiatractylenolide, were documented in the 1990s, several bioactive SDs with novel structures have been isolated from the *Atractylodes* genus only within the past three years [11-13]. Further investigation of the bioactive substances and their underlying mechanisms remains necessary.

This study reports the isolation of thirteen distinctive rearranged 9(8→7)-*abeo*-eudesmane-type SDs, atramacronins A–M (**1**–**13**), three eudesmane-type SDs, atramacronins N–P (**14**–**16**), and two known meroterpenoids, atrachinenin G (**17**) and atrachinenin I (**18**) (Fig. 1), from *A. macrocephala*. The cytotoxicity of compounds **1**–**7**, **9**–**14,** and **16**–**18** was evaluated against Hep3B, HepG2, and Huh7 cell lines. This paper details their structural elucidation and cytotoxic activities against these three liver cancer cell lines.

2. Results and discussion

Atramacronin A (**1**) was isolated as a colorless bulk crystal. The high-resolution electrospray ionization mass spectrometry (HR-ESI-MS) spectrum of compound **1** exhibited a quasi-molecular ion peak at *m*/*z* 519.2711, indicating a molecular formula of $C_{30}H_{40}O_6$ (Calcd. for $C_{30}H_{40}O_6Na^+$, 519.2718) with 11 degrees of unsaturation. The ^{1}H nuclear magnetic resonance (NMR) spectrum of **1** revealed signals for four methyl groups at δ_H 0.83 (3H, s), 0.97 (3H, s), 1.26 (3H, s), 1.87 (3H, s) and two exomethylene groups at δ_H 4.49 (1H, br s), 4.59 (1H, br s), 4.76 (1H, br s), 4.87

* Corresponding author.
E-mail addresses: mminchen@swu.edu.cn (M. Chen); mengfc@swu.edu.cn (F. Meng)

https://doi.org/10.1016/S1875-5364(26)61082-5

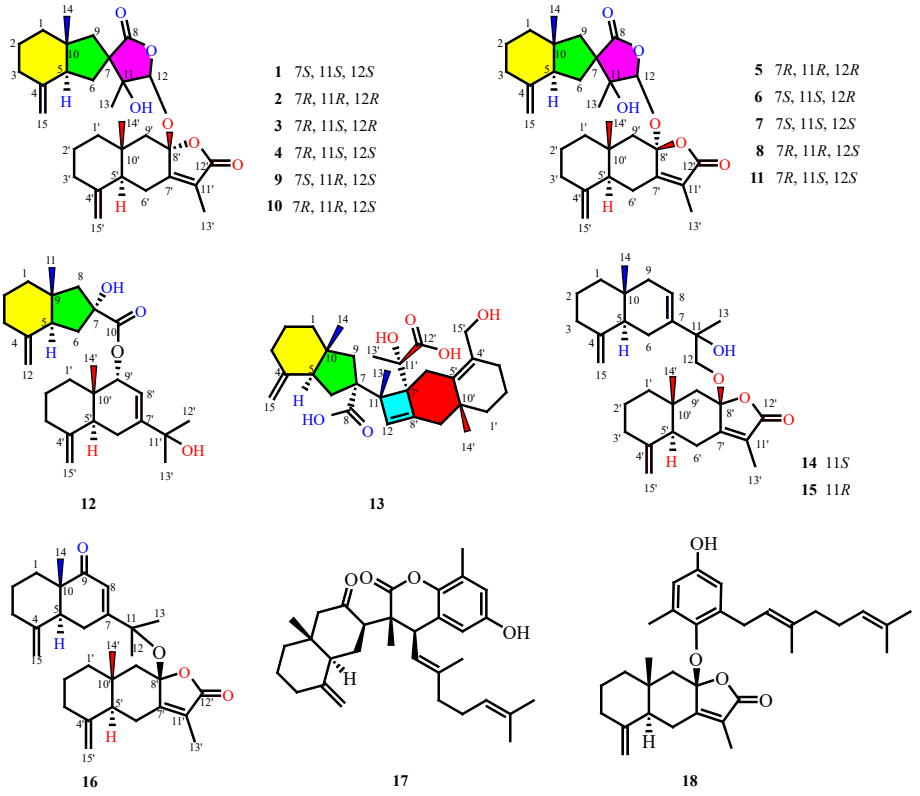

Fig. 1 Chemical structures of **1**–**18**.

(1H, br s). An acetal proton signal was observed at δ_H 5.37 (1H, s). Analysis of the ^{13}C NMR and heteronuclear single quantum correlation (HSQC) spectra revealed 30 carbons (Table 1) attributed to 11 quaternary carbons (δ_C 179.3, 171.1, 158.8, 148.8, 147.7, 124.7, 105.5, 79.7, 54.3, 43.7, 36.9), 3 methine carbons (δ_C 101.8, 53.7, 51.5), 12 methylene carbons (δ_C 107.1, 105.9, 49.4, 47.4, 41.2, 39.5, 36.1, 34.9, 29.7, 24.9, 23.4, 22.3) and 4 methyl carbons (δ_C 18.5, 17.6, 17.0, 8.6). The presence of characteristic signals for terminal methylene groups, methyl groups, and carboxyl of *α*-, *β*-unsaturated lactone suggested that compound **1** was likely a sesquiterpenoid dimer containing at least one eudesmanolide fragment.

The planar structure of compound **1** was determined through analysis of the heteronuclear multiple bond correlation (HMBC) and ^1H–^1H correlation spectroscopy (COSY) correlations (Fig. 2). An 8-oxygenated eudesmanolide portion, identical to atractylenolide III, was initially identified based on the HMBCs from H-13′ (δ_H 1.90) to C-7′ (δ_C 158.8), C-11′ (δ_C 124.7), C-12′ (δ_C 171.1), from H-14′ (δ_H 0.97) to C-1′ (δ_C 41.2), C-5′ (δ_C 51.5), C-9′ (δ_C 49.4), C-10′ (δ_C 36.9), from H-15′ (δ_H 4.87, 4.59) to C-3′ (δ_C 36.1), C-4′ (δ_C 148.8), C-5′ (δ_C 51.5), and the ^1H–^1H COSY correlations of H-1′/H-2′/H-3′. Additionally, another tetra-substituted six-membered ring containing an exocyclic double bond and a methyl was established through the HMBC cross-peaks of H-14/C-1, C-5, C-9, C-10, H-15/C-3, C-4, C-5 and the ^1H–^1H COSY correlations of H-1-H-2-H-3. The HMBCs between H-12 (δ_H 5.37) and C-7 (δ_C 54.3), C-8 (δ_C 179.3), C-11 (δ_C 79.7), between H-13 (δ_H 1.26) and C-7 (δ_C 54.3), C-11 (δ_C 79.7), C-12 (δ_C 101.8) indicated a 5-membered lactone ring with methyl and hydroxy substitutions at C-11. The HMBCs of H-6/C-8 and H-9/C-8 were also observed. These findings indicated the 9(8→7) rearranged structural fragment from an eudesmanolide. The C_{12}-O-$C_{8'}$ linkage between two sesquiterpenoid moieties was established based on the HMBC between H-12 (δ_H 5.37) and C-8′ (δ_C 105.5), thus completing the elucidation of compound **1**'s planar structure.

The relative configuration of compound **1** was established through analysis of its nuclear Overhauser effect spectroscopy (NOESY) spectrum (Fig. 3). The NOESY correlations of H-6/H-12, H-9/H-13 indicated the *β* orientations of H-12 and the *α* orientations of CH_3-13. Based on biogenetic considerations, H-5 and H-5′ were assigned as *α*-oriented, while 14-Me and 14′-Me were assigned as *β*-oriented. However, due to the spiral carbon atom of C-7, the relative configuration between H-5 and C-7 could not be determined from NOESY correlations. To establish its absolute configuration, calculations of the circular dichroism (CD) spectra and ^{13}C NMR chemical shifts of possible structures of **1** were conducted. $MAE_{\Delta\Delta\delta}$ (mean absolute error) analysis [14] of the calculated and experimental ^{13}C NMR data (Table S1) indicated that the configuration of **1** was 5*S**,7*S**,10*R**,11*S**,12*S**,5′*S**,8′*S**,10′*R**. Subsequently, the absolute configuration of **1** was determined as 5*S*,7*S*,10*R*,11*S*,12*S*,5′*S*,8′*S*,10′*R* through comparison of its experimental and calculated CD curves (Fig. S1). Finally, single-crystal X-ray diffraction analysis (Fig. 4) using Cu K*α* radiation definitively confirmed its absolute configuration.

Atramacronin B (**2**) was isolated as a colorless bulk crystal and determined to share the same molecular formula as compound **1**, $C_{30}H_{40}O_6$, based on its HR-ESI-MS data ($[M + Na]^+$ *m/z* 519.2712, Calcd. for $C_{30}H_{40}O_6Na^+$, 519.2718). Analysis of the 1D and 2D NMR data between **2** (Table 1) and **1** revealed an identical planar structure. The relative configuration of the newly formed 5-membered lactone ring in **2** was determined to be identical to that of **1** based on the NOE correlations of H-6/H-12, H-9/H-13 in the NOESY spectrum of **2** (Fig. 3). Compound **2** was hypothesized to possess a different relative configuration between H-5 and C-7. $MAE_{\Delta\Delta\delta}$ analysis of the experimental and calculated ^{13}C NMR data (Table S1) and comparison of the CD spectra (Fig. S1) established the absolute configuration of **2** as 5*S*,7*R*,10*R*,11*R*,12*R*,5′*S*,8′*S*,10′*R*. The structural assignment and absolute configuration were further validated *via* single-crystal X-ray diffraction (Fig. 4).

Atramacronin C (**3**), obtained as a colorless bulk crystal, shared the molecular formula $C_{30}H_{40}O_6$ with compounds **1** and **2**,

Table 1 ^{1}H (400 MHz) and ^{13}C (100 MHz) NMR data of atramacronins A–F (**1**–**6**) in $CDCl_3$.

No.	Type	1		2		3		4		5		6	
		δ_C	δ_H (*J* in Hz)	δ_C	δ_H (*J* in Hz)	δ_C	δ_H (*J* in Hz)	δ_C	δ_H (*J* in Hz)	δ_C	δ_H (*J* in Hz)	δ_C	δ_H (*J* in Hz)
1	CH_2	39.5	1.74 m 1.27 m	39.0	1.68 m 1.39 m	39.0	1.73 m 1.45 m	38.9	1.73 m 1.44 m	39.0	1.71 m 1.43 m	39.7	1.83 m 1.30 m
2	CH_2	23.4	1.62 m	23.6	1.66 m 1.60 m	23.7	1.67 m 1.60 m	23.7	1.65 m 1.59 m	23.7	1.64 m	23.3	1.61 m 1.46 m
3	CH_2	34.9	2.27 m 1.92 m	34.7	2.26 dd (13.9, 4.1) 2.00 m	34.7	2.25 dd (14.2, 4.0) 1.97 m	34.7	2.24 m 1.97 m	34.7	2.26 m 2.03 m	35.0	2.28 m 2.00 m
4	C	147.7		147.9		147.9		148.3		148.0		147.9	
5	CH	53.7	1.92 m	51.7	2.45 m	51.6	2.36 m	51.9	2.39 m	51.6	2.47 m	53.6	1.89 m
6	CH_2	29.7	2.14 m 2.03 m	30.5	1.94 m 1.86 m	32.3	1.78 m 1.65 m	33.2	1.84 m 1.72 m	30.4	1.98 m 1.89 m	34.7	2.05 m 1.89 m
7	C	54.3		54.2		54.8		54.7		54.4		53.6	
8	C	179.3		181.4		180.1		180.1		180.7		180.7	
9	CH_2	47.4	1.90 m 1.59 m	47.9	1.89 m 1.68 m	44.8	2.00 d (13.7) 1.80 d (13.7)	43.5	1.99 m 1.78 m	47.2	1.86 m 1.78 m	43.8	1.97 d (13.4) 1.64 d (13.4)
10	C	43.7		43.3		42.7		42.3		43.2		42.3	
11	C	79.7		79.4		77.0		79.3		79.6		80.2	
12	CH	101.8	5.37 s	100.6	4.94 s	98.1	4.88 s	102.0	5.35 s	102.2	5.40 s	102.6	5.44 s
13	CH_3	18.5	1.26 s	19.2	1.39 s	20.7	1.30 s	18.5	1.30 s	19.2	1.29 s	18.0	1.25 s
14	CH_3	17.0	0.83 s	18.7	0.70 s	18.8	0.71 s	17.0	0.97 s	18.7	0.68 s	17.6	0.90 s
15	CH_2	105.9	4.76 br s 4.49 br s	105.5	4.74 br s 4.46 br s	105.5	4.74 br s 4.40 br s	105.1	4.72 br s 4.38 br s	105.5	4.75 d (1.4) 4.45 d (1.4)	105.7	4.75 br s 4.37 br s
1′	CH_2	41.2	1.60 m 1.24 m	41.2	1.56 m 1.22 m	41.2	1.59 m 1.25 m	41.2	1. 62 m 1.24 m	42.3	1.64 m	42.8	1.64 m
2′	CH_2	22.3	1.62 m	22.4	1.62 m	22.4	1.64 m	22.3	1.63 m	23.3	1.69 m	23.5	1.66 m
3′	CH_2	36.1	2.44 m 1.94 m	36.1	2.36 m 1.94 m	36.1	2.39 m 1.94 m	36.1	2.36 m 1.95 m	36.7	2.45 m 2.05 m	36.7	2.39 m 2.06 m
4′	C	148.8		148.0		147.9		148.4		148.3		148.2	
5′	CH	51.5	1.85 m	52.1	1.82 m	52.1	1.84 m	51.5	1.84. m	41.6	2.65 m	41.6	2.65 m
6′	CH_2	24.9	2.68 dd (13.3, 3.0) 2.36 m	25.5	2.68 dd (13.4, 3.2) 2.53 br d (13.4)	25.5	2.70 dd (13.4, 3.2) 2.54 dd (13.4, 13.4)	24.9	2.64 dd (13.2, 2.8) 2.32 m	23.8	2.66 m 2.57 m	23.8	2.67 m 2.50 m
7′	C	158.8		160.2		160.2		158.9		156.7		156.8	
8′	C	105.5		105.6		105.5		105.5		106.1		106.0	
9′	CH_2	49.4	2.51 d (14.2) 1.48 d (14.2)	51.6	2.33 d (13.7) 1.52 d (13.7)	51.6	2.39 d (13.8) 1.55 d (13.8)	49.4	2.51 d (14.2) 1.49 d (14.2)	47.9	2.51d (14.8) 1.81 d (14.8)	47.7	2.53 d (14.1) 1.78 d (14.1)
10′	C	36.9		36.9		36.9		36.9		35.3		35.3	
11′	C	124.7		125.5		125.4		124.6		125.5		125.4	
12′	C	171.1		171.3		171.0		171.1		171.4		171.4	
13′	CH_3	8.6	1.87 s	8.6	1.88 s	8.7	1.90 s	8.6	1.87 s	8.7	1.90 s	8.7	1.88 s
14′	CH_3	17.6	0.97 s	17.4	0.90 s	17.4	0.95 s	17.0	0.97 s	21.2	0.68 s	21.2	0.67 s
15′	CH_2	107.1	4.87 br s 4.59 br s	107.6	4.86 br s 4.63 br s	107.7	4.88 br s 4.64 br s	107.2	4.86 br s 4.58 br s	107.7	4.90 br s 4.64 br s	107.7	4.90 m 4.64 m

as confirmed by HR-ESI-MS data ($[M + NH_4]^+$ *m/z* 514.3168, Calcd. for $C_{30}H_{44}O_6N^+$, 514.3164). Analysis of its 1D and 2D NMR data (Table 1) established an identical planar structure. The ROESY spectrum of **3** revealed ROE correlations of H-6/H-12/H-13, indicating a different absolute configuration in the lactone ring. The absolute configuration of **3** was determined as 5*S*,7*R*,10*R*,11*S*,12*R*,5′*S*,8′*S*,10′*R* through $MAE_{\Delta\Delta\delta}$ analysis of the experimental and calculated ^{13}C NMR data (Table S2) and comparison of its CD spectrum (Fig. S1) with calculated spectra. Single-crystal X-ray diffraction analysis confirmed this structural assignment (Fig. 4).

Atramacronin D (**4**) exhibited an identical planar structure to compounds **1**–**3**, as evidenced by HR-ESI-MS data ($[M + Na]^+$ *m/z* 519.2708, Calcd. for $C_{30}H_{40}O_6Na^+$, 519.2718) and 1D and 2D NMR data (Table 1). NOE correlations of H-6/H-13 and H-9/H-12 indicated similar orientations of these respective proton pairs. The absolute configuration of **4** was established as 5*S*,7*R*,10*R*,11*S*,12*S*,5′*S*,8′*S*,10′*R* through DP4+ analysis of the experimental and calculated ^{13}C NMR data (Table S3) and comparison of its CD spectrum (Fig. S1) with calculated spectra. Single-crystal X-ray diffraction analysis provided unambiguous confirmation of this configuration (Fig. 4).

Atramacronin E (**5**) and F (**6**) exhibited sodium-adductive molecular ion peaks at *m/z* 519.2712 in their HR-ESI-MS spectra, indicating identical molecular formulas. Analysis of their 1D and 2D NMR data revealed the same planar structure as compounds **1**–**4**. Detailed examination of their ^{1}H and ^{13}C NMR data (Table 1) showed notable differences in chemical shifts of H-5′, C-5′, and C-10′. For compounds **5** and **6**, the chemical shifts of H-5′, C-5′, and C-10′ were 2.65, 41.6, and 51.3, respectively, while in compounds **1**–**4** these values were 1.82–1.85, 51.5–52.1, and 36.9, respectively. A similar pattern was observed in biatractylenolide (8*S*, $\delta_{H\text{-}5}$ 2.82, $\delta_{C\text{-}5}$ 53.2) and biepiatractylenolide (8*R*, $\delta_{H\text{-}5}$ 1.70, $\delta_{C\text{-}5}$ 42.9) [15], which possess different absolute configurations at C-8. This evidence suggested that compounds **5** and **6** have the opposite 8′*R* configuration compared to compounds **1**–**4**. The NOE correlations of H-6/H-12, H-9/H-13 in the ROESY spectrum of **5** (Fig. 3) indicated an identical relative configuration of the newly-formed 5-membered lactone ring with compounds **1** and **2**. The NOE correlations of H-9/H-12/H-13 in the NOESY spectrum of **6** (Fig. 3) demonstrated the same orientation of H-9,12,13. Through comparison of its CD spectrum with calculated ones (Fig. S1) and

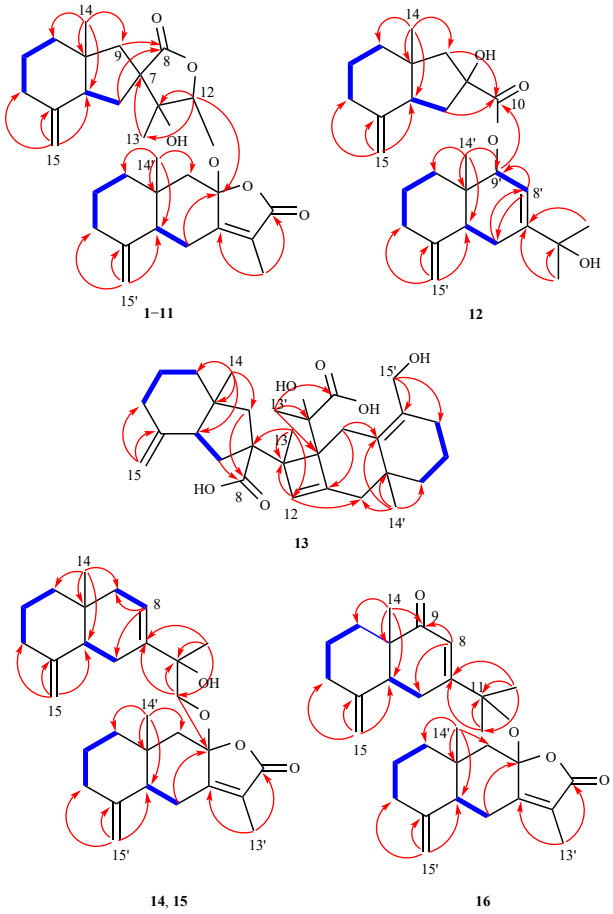

Fig. 2 Key HMBC (⟶) and ^{1}H–^{1}H COSY (▬) correlations of compounds **1**–**16**.

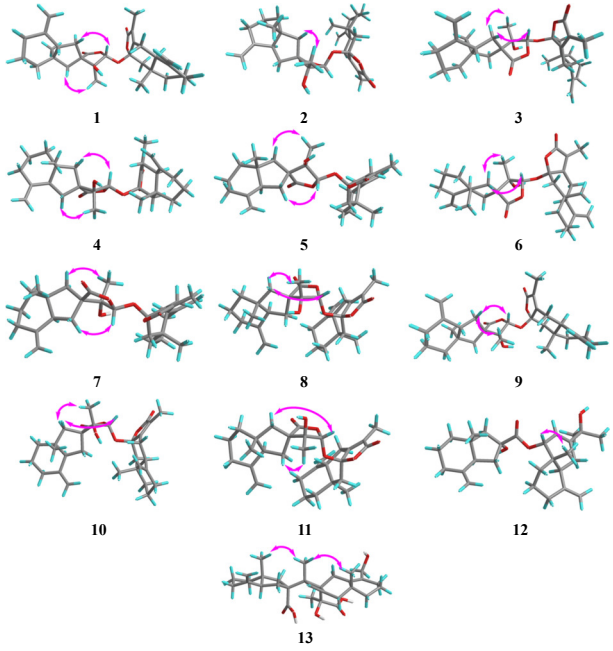

Fig. 3 Key NOE (⟷) correlations of compounds **1**–**13**.

$MAE_{\Delta\Delta\delta}$ analysis of experimental and calculated NMR data (Tables S4 and S5), the absolute configuration of **5** was determined as 5*S*,7*R*,10*R*,11*R*,12*R*,5′*S*,8′*R*,10′*R* and that of **6** as 5*S*,7*S*,10*R*,11*S*,12*R*,5′*S*,8′*R*,10′*R*.

Atramacronins G–K (**7**–**11**) were isolated as white amorphous powders and shared the molecular formula $C_{30}H_{40}O_6$ with compounds **1**–**6**, as evidenced by their HR-ESI-MS data (Table 2). Their identical planar structures were established through analysis of 1D and 2D NMR data. The absolute configurations at C-8′ were determined to be *R* for compounds **7**, **8**, and **11**, while compounds **9** and **10** possessed the 8′*S* configuration.

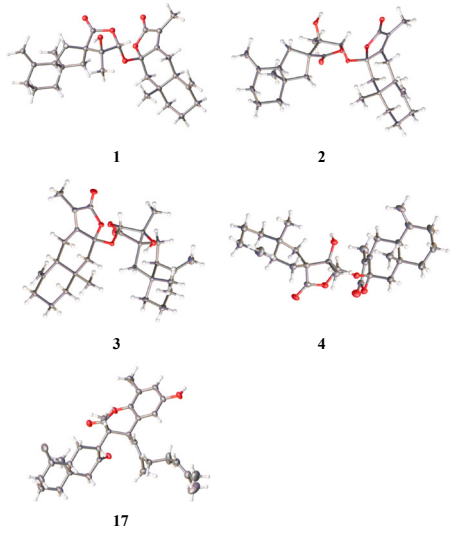

Fig. 4 X-ray crystallographic analysis of compounds **1**–**4** and **17**.

For compound **7**, identical orientations of H-6/H-12 and H-9/H-13 were determined based on the NOE correlations of H-6/H-12 and H-9/H-13 in its NOESY spectrum (Fig. 3). Through $MAE_{\Delta\Delta\delta}$ analysis of the experimental and calculated ^{13}C NMR data (Table S4) and comparison of its CD spectrum (Fig. S1) with the calculated spectra, the absolute configuration of **7** was established as 5*S*,7*S*,10*R*,11*S*,12*S*,5′*S*,8′*R*,10′*R*, named as atramacronin G.

In the ROESY spectrum of **8** (Fig. 3), the NOE correlations of H-9/H-12/H-13 indicated identical relative configurations in the lactone ring with **6**. Through $MAE_{\Delta\Delta\delta}$ analysis of the experimental and calculated ^{13}C NMR data (Table S5) and comparison of its CD spectrum (Fig. S1) with the calculated spectra, the absolute configuration of **8** was determined as 5*S*,7*R*,10*R*,11*R*,12*S*,5′*S*,8′*R*,10′*R*, named as atramacronin H.

The NOE correlations of H-6/H-12/H-13 in the NOESY spectrum of **9** (Fig. 3) indicated identical relative configurations in the lactone ring with **3**. Through $MAE_{\Delta\Delta\delta}$ analysis of the experimental and calculated ^{13}C NMR data (Table S2) and comparison of its CD spectrum (Fig. S1) with the calculated spectra, the absolute configuration of **9** was established as 5*S*,7*S*,10*R*,11*R*,12*S*,5′*S*,8′*S*,10′*R*, named as atramacronin I.

The identical orientations of H-9/H-12/H-13 in compound **10** were confirmed by the NOE correlations of H-9/H-12/H-13 in its ROESY spectrum (Fig. 3). Through DP4+ analysis of the experimental and calculated ^{13}C NMR data (Table S6) and comparison of its CD spectrum (Fig. S1) with the calculated spectra, the absolute configuration of **10** was determined as 5*S*,7*R*,10*R*,11*R*,12*S*,5′*S*,8′*S*,10′*R*, named as atramacronin J.

The NOE correlations of H-6/H-13, H-9/H-12 in the NOESY spectrum of **11** (Fig. 3) demonstrated identical orientations of H-6/H-13 and H-9/H-12, respectively. Through DP4+ analysis of the experimental and calculated ^{13}C NMR data (Table S7) and comparison of its CD spectrum (Fig. S1) with the calculated spectra, the absolute configuration of **11** was established as 5*S*,7*R*,10*R*,11*S*,12*S*,5′*S*,8′*R*,10′*R*, named as atramacronin K.

Atramacronin L (**12**), isolated as a white amorphous powder, exhibits a molecular formula of $C_{27}H_{40}O_4$ as determined by the quasi-molecular ion peak at *m*/*z* 451.2813 $[M + Na]^+$ (Calcd. for $C_{27}H_{40}O_4Na^+$, 451.2819) in its HR-ESI-MS spectrum, indicating 8 degrees of unsaturation. The ^{1}H NMR spectrum of **12** (Table 3)

Table 2 ^{1}H (400 MHz) and ^{13}C (100 MHz) NMR data of atramacronins G–K (**7**–**11**) in $CDCl_3$.

No.	Type	**7**		**8**		**9**		**10**		**11**	
		δ_C	δ_H (J in Hz)	δ_C	δ_H (J in Hz)	δ_C	δ_H (J in Hz)	δ_C	δ_H (J in Hz)	δ_C	δ_H (J in Hz)
1	CH_2	39.6	1.76 m 1.31 m	38.9	1.73 m 1.43 m	39.6	1.81 m 1.31 m	38.9	1.73 m 1.44 m	38.9	1.75 m 1.49 m
2	CH_2	23.4	1.64 m	23.6	1.67 m	23.5	1.66 m	23.7	1.71 m 1.62 m	23.3	1.62 m 1.44 m
3	CH_2	35.1	2.29 m 1.93 m	34.7	2.57 m 2.00 m	34.8	2.28 m 1.93 m	34.8	2.26 dd (14.4, 4.4) 2.01 m	34.6	2.36 dd (13.5, 5.4) 2.01 dd (13.5, 6.5)
4	C	147.6	-	148.1	-	147.9	-	148.2	-	148.3	-
5	CH	53.7	1.96 m	52.0	2.34 m	53.6	1.94 m	51.9	2.39 m	51.9	2.38 m
6	CH_2	29.6	2.14 dd (12.4, 5.9) 2.04 dd (12.4, 12.4)	32.5	2.03 dd (13.0, 13.0) 1.87 dd (13.0, 5.8)	35.5	2.14 dd (11.8, 4.5) 1.85 m	31.7	1.92 m 1.89 m	34.4	1.86 m 1.84 m
7	C	54.3	-	54.1	-	53.4	-	53.9	-	54.7	-
8	C	179.6	-	179.9	-	181.4	-	179.7	-	180.4	-
9	CH_2	48.5	1.85 d (13.4) 1.72 d (13.4)	45.2	1.79 d (13.3) 1.76 d (13.3)	43.7	1.95 d (13.6) 1.65 m	45.1	1.79 m	43.4	1.96 d (13.5) 1.80 d (13.5)
10	C	43.8	-	43.1	-	42.6	-	43.0	-	41.9	-
11	C	79.5	-	76.8	-	80.0	-	77.0	-	79.3	-
12	CH	99.8	4.94 s	97.6	4.85 s	100.9	4.95 s	99.9	5.35 s	100.0	4.92 s
13	CH_3	18.6	1.36 s	22.1	1.29 s	17.4	1.36 s	22.2	1.28 s	18.6	1.41 s
14	CH_3	17.8	0.84 s	18.4	0.72 s	17.4	0.89 s	18.6	0.70 s	19.1	0.71 s
15	CH_2	106.0	4.78 br s 4.51 br s	105.6	4.75 br s 4.44 br s	105.7	4.73 br s 4.30 br s	105.4	4.75 br s 4.43 br s	105.0	4.74 d (1.8) 4.39 d (1.8)
1′	CH_2	43.1	1.67 m 1.40 m	43.0	1.70 m 1.43 m	41.1	1.57 m 1.22 m	41.2	1.66 m 1.26 m	43.2	1.68 m 1.39 m
2′	CH_2	23.4	1.64 m 1.46 m	23.3	1.67 m 1.46 m	22.4	1.63 m	22.3	1.66 m	23.7	1.65 m 1.62 m
3′	CH_2	36.7	2.38 m 1.95 m	36.6	2.35 m 1.99 m	36.1	2.36 m 1.95 m	36.1	2.37 m 1.98 m	36.7	2.36 m 1.93 m
4′	C	147.5	-	147.5	-	147.9	-	148.2	-	147.5	-
5′	CH	41.8	2.59 dd (11.7, 11.7)	41.9	2.63 m	52.0	1.83 m	51.5	1.85 m	42.2	2.62 dd (11.3, 11.3)
6′	CH_2	24.4	2.74 m 2.62 m	24.4	2.75 m 2.64 m	25.5	2.69 dd (13.4, 3.2) 2.53 dd (13.4, 13.4)	24.9	2.69 dd (13.2, 3.0) 2.37 m	24.4	2.74 m 2.63 m
7′	C	158.3	-	158.3	-	160.3	-	158.8	-	158.3	-
8′	C	105.7	-	105.3	-	105.5	-	105.4	-	105.6	-
9′	CH_2	50.8	2.21 d (14.8) 1.86 d (14.8)	50.8	2.56 d (14.8) 1.93 d (14.8)	51.6	2.31 d (13.9) 1.52 d (13.9)	49.3	2.56 d (14.3) 1.53 d (14.3)	50.8	2.22 d (14.9) 1.87 d (14.9)
10′	C	34.9	-	35.1	-	36.9	-	36.9	-	35.1	-
11′	C	126.3	-	126.3	-	125.5	-	124.7	-	126.2	-
12′	C	171.4	-	171.1	-	171.5	-	170.7	-	171.4	-
13′	CH_3	8.7	1.90 s	8.8	1.91 s	8.6	1.87 s	8.6	1.90 s	8.7	1.90 s
14′	CH_3	21.2	0.66 s	21.1	0.66 s	17.9	0.94 s	17.2	1.00 s	21.2	0.66 s
15′	CH_2	108.3	4.89 br s 4.65 br s	108.3	4.89 br s 4.65 br s	107.6	4.87 br s 4.64 br s	107.3	4.88 br s 4.59 br s	108.3	4.88 br s 4.64 br s

revealed four methyls at δ_H 1.36 (6H, s, H-12′, 13′), 0.91 (3H, s, H-11), 0.76 (3H, s, H-14′) and five olefinic proton signals at δ_H 5.86 (1H, dd, J = 5.4, 2.0 Hz, H-8′), 4.92 (1H, d, J = 5.4 Hz, H-9′), 4.88 (1H, d, J = 1.4 Hz, H-15′a), 4.77 (1H, d, J = 1.3 Hz, H-12a), 4.47 (1H, d, J = 1.3 Hz, H-12b). Analysis of the ^{13}C NMR and HSQC spectra indicated the presence of 27 carbon signals corresponding to 4 methyls, 11 methylenes, 4 methines, and 8 quaternary carbons, including one ester carbonyl carbon (δ_C 177.7), three double bonds (δ_C 150.6, 149.3, 147.9, 114.6, 107.7, 105.6), two oxygenated quaternary carbons (δ_C 79.7, 73.0) and one oxygenated methine (δ_C 76.6). The planar structure of **12** was established through analysis of the HMBC data (Fig. 2). A C-9′/11′ oxygen-substituted eudesmane scaffold containing two double bonds at $C_{4'}$=$C_{15'}$ and $C_{7'}$=$C_{8'}$ was established based on the HMBCs between H-14′ and C-1′, 5′, 9′, 10′, between H-15′ and C-3′, 4′, 5′, between H-12′/13′ and C-7′, 1′, between H-9′ and C-5′, 7′, 8′, 10′, 14′. The correlations from H-11 to C-1, 5, 9, 10, from H-12 to C-3, 4, 5, and from H-6 to C-4, 5, 7, 9, 10 indicated a 6/5 bicyclic fragment with an exocyclic double bond at C_4=C_{12}, a methyl at C-9, and a carbonyl at oxygenated C-8. The connection between C-10 and C-9′ *via* an ester bond was established by the HMBC between H-9′ and C-10. Consequently, the planar structure of **12** was determined to be a dimer comprising one eudesmane-type sesquiterpenoid and one rearranged norsesquiterpenoid. The relative configuration of **12** was established through analysis of the ROESY correlations (Fig. 3). The correlation from H-9′ to H-14′ indicated the same orientation of H-9 and 14′-Me. Based on biogenetic considerations, H-5 and H-5′ were assigned as *α*-oriented, while 11-Me and 14′-Me were assigned as *β*-oriented. The relative configuration of C-7 could not be determined solely from NOESY correlations. The absolute configuration was established by comparing the experimental CD spectrum of **12** with calculated spectra of possible structures (Fig. S1). The CD curve matched that of 5*S*,7*R*,9*R*,5′*S*,9′*R*,10′*R*-**12**. Therefore, the absolute configuration of **12** was established as 5*S*,7*R*,9*R*,5′*S*,9′*R*,10′*R*.

Atramacronin M (**13**) was isolated as a white amorphous powder. Its HR-ESI-MS spectrum exhibited sodium-adductive quasi-molecular ion peaks at m/z 521.2867 (Calcd. for

Table 3 ^{1}H (400 MHz) and ^{13}C (100 MHz) NMR data of atramacronins L–P (**12**–**16**) in $CDCl_3$.

No.	12		13		14		15		16	
	δ_C	δ_H (*J* in Hz)	δ_C	δ_H (*J* in Hz)	δ_C	δ_H (*J* in Hz)	δ_C	δ_H (*J* in Hz)	δ_C	δ_H (*J* in Hz)
1	39.8, CH_2	2.21 m 1.73 m	38.6, CH_2	1.74 m 1.37 m	41.7, CH_2	1.55 m 1.21 m	41.7, CH_2	1.57 m 1.32 m	32.7, CH_2	2.03 m 1.54 m
2	23.4, CH_2	1.67 m	23.5, CH_2	1.64 m	23.7, CH_2	1.55 m	23.8, CH_2	1.62 m 1.58 m	23.0, CH_2	1.76 m 1.60 m
3	35.2, CH_2	2.28 m 1.91 m	34.6, CH_2	2.32 m 2.01 m	37.3, CH_2	2.37 m 2.00 m	37.4, CH_2	2.37 m 1.99 m	36.2, CH_2	2.34 m 2.08 m
4	147.9, C	-	147.6, C	-	150.1, C	-	150.0, C	-	149.2, C	-
5	54.3, CH	2.28 m	52.2, CH	2.55 dd (12.5, 6.1)	45.0, CH	1.96 m	45.0, CH	1.98 m	45.6, CH	2.82 dd (11.3, 3.2)
6	39.5, CH_2	2.03 m 1.20 m	32.4, CH_2	2.36 m 1.89 dd (12.5, 12.5)	24.9, CH_2	1.95 m 1.91 m	24.9, CH_2	2.03 m 1.96 m	25.4, CH_2	2.62 dd (17.6, 3.2) 2.22 m
7	79.7, C	-	58.9, C	-	138.4, C	-	139.4, C	-	164.8, C	-
8	55.2, CH_2	1.85 d (13.0) 1.77 d (13.0)	180.5, C	-	120.0, CH	5.68 br s	119.3, CH	5.68 br s	121.5, CH	5.68 d (2.4)
9	43.6, C	-	50.4, CH_2	2.34 m 1.67 m	42.0, CH_2	1.91 m	42.1, CH_2	1.93 m	205.4, C	-
10	177.7, C	-	43.3, C	-	34.3, C	-	34.4, C	-	45.9, C	-
11	18.0, CH_3	0.91 s	56.5, C	-	74.0, C	-	74.2, C	-	79.0, C	-
12	105.6, CH_2	4.77 d (1.3) 4.47 d (1.3)	112.8, CH	5.53 s	68.9, CH_2	3.29 d (8.9) 3.20 d (8.9)	69.1, CH_2	3.47 d (12.9) 3.02 d (12.9)	29.7, CH_3	1.41 s
13	-	-	19.1, CH_3	1.52 s	24.2, CH_3	1.25 s	24.3, CH_3	1.22 s	26.0, CH_3	1.39 s
14	-	-	18.2, CH_3	0.70 s	17.3, CH_3	0.66 s	17.3, CH_3	0.69 s	15.5, CH_3	0.88 s
15	-	-	105.2, CH_2	4.79 d (1.2) 4.44 d (1.2)	106.5, CH_2	4.79 d (1.1) 4.55 d (1.1)	106.8, CH_2	4.81 d (1.1) 4.61 d (1.1)	107.6, CH_2	4.91 d (1.4) 4.68 d (1.4)
1′	34.3, CH_2	1.64 m 1.31 m	39.8, CH_2	1.57 m 1.28 m	41.4, CH_2	1.55 m 1.21 m	41.3, CH_2	1.57 m 1.21 m	41.3, CH_2	1.55 m 1.15 m
2′	23.6, CH_2	1.65 m	18.2, CH_2	1.58 m	22.5, CH_2	1.62 m	22.5, CH_2	1.62 m	22.4, CH_2	1.89 m 1.64 m
3′	37.2, CH_2	2.37 m 1.93 m	31.9, CH_2	2.19 m 1.90 m	36.2, CH_2	2.33 m 1.94 m	36.2, CH_2	2.34 m 1.95 m	36.2, CH_2	2.34 m 1.96 m
4′	149.3, C	-	127.1, C	-	148.7, C	-	148.6, C	-	148.8, C	-
5′	40.0, CH	2.31 m	139.8, C	-	52.0, CH	1.80 br d (12.4)	52.0, CH	1.82 br d (11.8)	52.5, CH	1.76 m
6′	25.2, CH_2	2.26 m 2.09 m	28.0, CH_2	3.20 d (15.5) 2.35 d (15.5)	25.0, CH_2	2.58 dd (12.9, 3.1) 2.17 m	25.1, CH_2	2.62 dd (13.1, 3.2) 2.24 m	26.0, CH_2	2.66 dd (16.8, 3.2) 2.41 m
7′	150.6, C	-	61.5, C	-	159.4, C	-	159.4, C	-	161.5, C	-
8′	114.6, CH	5.86 dd (5.4, 2.0)	118.6, C	-	105.9, C	-	106.0, C	-	105.9, C	-
9′	76.6, CH	4.92 d (5.4)	48.3, CH_2	2.40 d (14.1) 2.09 d (14.1)	51.2, CH_2	2.33 d (13.6) 1.45 d (13.6)	51.1, CH_2	2.27 d (13.7) 1.45 d (13.7)	54.5, CH_2	2.35 d (13.5) 1.29 d (13.5)
10′	37.9, C	-	34.1, C	-	36.9, C	-	36.9, C	-	36.9, C	-
11′	73.0, C	-	81.5, C	-	124.5, C	-	124.5, C	-	124.0, C	-
12′	29.4, CH_3	1.36 s	173.4, C	-	171.5, C	-	171.6, C	-	171.0, C	-
13′	29.1, CH_3	1.36 s	21.1, CH_3	1.70 s	8.5, CH_3	1.86 s	8.5, CH_3	1.87 s	8.4, CH_3	1.78 s
14′	16.4, CH_3	0.76 s	24.7, CH_3	1.23 s	17.0, CH_3	0.94 s	17.1, CH_3	0.94 s	16.9, CH_3	1.00 s
15′	107.7, CH_2	4.88 d (1.4) 4.67 d (1.4)	64.2, CH_2	4.57 d (11.3) 3.77 d (11.3)	106.8, CH_2	4.84 d (1.0) 4.52 d (1.0)	107.0, CH_2	4.85 d (1.0) 4.57 d (1.0)	106.8, CH_2	4.86 d (1.2) 4.59 d (1.2)

$C_{30}H_{42}O_6Na^+$, 521.2874), indicating the molecular formula of $C_{30}H_{42}O_6$. The ^{1}H NMR spectrum of **13** (Table 3) revealed signals of three olefinic protons at δ_H 5.53 (1H, s), 4.79 (1H, d, *J* = 1.2 Hz), 4.44 (1H, d, *J* = 1.2 Hz), one set of oxygenated methylene protons at δ_H 4.57 (1H, d, *J* = 11.3 Hz), 3.77 (1H, d, *J* = 11.3 Hz), and four methyl groups at δ_H 1.70 (3H, s), 1.52 (3H, s), 1.23 (3H, s), 0.70 (3H, s). The ^{13}C NMR spectrum displayed 30 carbon signals. Analysis of the HSQC data enabled assignment of these 30 carbons as two carboxyl (δ_C 180.5, 173.4), three groups of double bonds (δ_C 147.6, 139.8, 127.1, 118.6, 112.8, 105.2), six quaternary carbons (δ_C 81.5, 61.5, 58.9, 56.5, 43.3, 34.1), one methine carbon at δ_C 52.2, 11 methylene carbons (δ_C 64.4, 50.4, 48.3, 39.8, 38.6, 34.6, 32.4, 31.9, 28.0, 23.5, 18.2), and four methyl carbons (δ_C 24.7, 21.1, 19.1, 18.2). The planar structure determination was accomplished through analysis of HMBC and ^{1}H–^{1}H COSY data (Fig. 2). A rearranged 6/5 bicyclic fragment identical to the previous 12 compounds was established based on HMBCs between H-14 and C-1, 5, 9, 10, between H-15 and C-3, 4, 5, between H-6, 9 and C-7, 8, between H-13 and C-11, 7. HMBCs from H-14′ to C-1′, 5′, 9′, 10′, and from H-15′ to C-3′, 4′, 5′, indicated the presence of a hydroxy group at C-15′ and a double bond between C-4′ and C-5′ in a eudesmane skeletal motif. Cross peaks from H-13′ to C-7′, 11′, 12′, from H-12 to C-7, 11, 7′, and from H-13 to C-7′, suggested a newly formed four-membered ring linked by C_{11}–$C_{7'}$ and C_{12}=$C_{8'}$. The chemical shifts of C-11′ (δ_C 81.5) and 12′ (δ_C 173.4) indicated hydroxyl substitution at C-11′ and carboxyl form at C-12′. The planar structure of **13** was consequently elucidated and is proposed to originate from a rearranged eudesmane skeleton, likely formed *via* a [2 + 2] cycloaddition reaction involving a eudesmane precursor. The relative configurations were established through NOE data analysis. Biogenetically, 14-Me and 14′-Me were assigned as *β*-oriented, and H-5 as *α*-oriented. NOE correla-

tions (Fig. 3) between H-13 and H-14, 14′ indicated *β*-orientation of Me-13 and *α*-orientation of 8-COOH. Considering the steric effects of the three carbon substituents attached to C-7′, this center was assigned an *α*-orientation. The relative configuration at C-11′ was determined using DP4+ probability analysis by comparing the experimental and calculated ^{13}C NMR chemical shifts (Table S8). The absolute configuration of **13** was established as 5*S*,7*R*,10*R*,11*S*,7′*R*,10′*R*,11′*S* through comparison of its CD spectrum with calculated ones (Fig. S1).

Atramacronin N (**14**) and O (**15**) exhibited identical planar structures, as evidenced by their quasi-molecular ion peaks at *m/z* 489.2963 (**14**), 489.2964 (**15**) [M + Na]$^+$ (Calcd. for $C_{30}H_{42}O_4Na^+$, 489.2976) in their HR-ESI-MS spectra and their NMR data (Table 3). The ^{1}H and ^{13}C NMR data of **14** and **15** demonstrated high similarity with minor variations. Their ^{1}H NMR spectra revealed signals characteristic of four methyl groups, two exomethylene groups, an olefinic proton, and one oxygenated methylene. Their ^{13}C NMR and HSQC spectra displayed comparable 30 carbon signals, categorized as 10 quaternary carbons, 3 methine carbons, 13 methylene carbons, and 4 methyl carbons. These spectral features aligned closely with those of atractylenolide III and selina-4(14),7-dien-11-ol [16], except for the chemical shifts at C-8 in atractylenolide III and C-12 in selina-4(14),7-dien-11-ol, indicating that **14** and **15** might be their adductive derivatives. The planar structure was established through analysis of HMBC and ^{1}H–^{1}H COSY correlations (Fig. 2). The atractylenolide III fragment was confirmed by HMBCs of H-13′/C-7′, 11′, 12′, H-14′/C-1′, 5′, 9′, 10′, H-15′/C-3′, 4′, 5′ and ^{1}H–^{1}H COSY correlations of H-1′/H-2′/H-3′. The selina-4(14),7-dien-11-ol fragment was verified through HMBCs from H-8 to C-6, 7, 9, 11, from H-12, H-13 to C-7, 11, from H-14 to C-1, 5, 9, 10, from H-15 to C-3, 4, 5. The connection between atractylenolide III and selina-4(14),7-dien-11-ol *via* C_{12}-O-$C_{8'}$ was established by HMBCs between H-12 and C-8′. Biogenetically, H-5 and H-5′ were assigned as *α*-oriented, while 14-Me and 14′-Me were designated as *β*-oriented. C-8′ was determined as *S* configuration based on the chemical shifts of C-5′ (δ_C 52.0) and C-10′ (δ_C 36.9). Subsequently, the absolute configurations of **14** and **15** were established as 5*S*,10*R*,11*S*,5′*S*,8′*S*,10′*R* and 5*S*,10*R*,11*R*,5′*S*,8′*S*,10′*R*, respectively, through $MAE_{\Delta\Delta\delta}$ analysis of the experimental and calculated ^{13}C NMR data (Table S9) and comparison of its CD spectrum (Fig. S1) with the calculated ones.

Atramacronin P (**16**), isolated as a white amorphous powder, exhibits a molecular formula of $C_{30}H_{40}O_4$ as determined by the quasi-molecular ion peak at *m/z* 487.2805 [M + Na]$^+$ (Calcd. for $C_{30}H_{40}O_4Na^+$, 487.2819) in its HR-ESI-MS spectrum, indicating 11 degrees of unsaturation. The ^{1}H NMR spectrum of **16** revealed signals of five methyl groups at δ_H 0.88 (3H, s), 1.00 (3H, s), 1.39 (3H, s), 1.41 (3H, s), 1.78 (3H, s), two exomethylene groups at δ_H 4.59 (1H, d, *J* = 1.2 Hz), 4.68 (1H, d, *J* = 1.4 Hz), 4.86 (1H, d, *J* = 1.2 Hz), 4.91 (1H, d, *J* = 1.4 Hz) and an olefinic proton at δ_H 5.68 (1H, d, *J* = 2.4 Hz). The ^{13}C NMR and HSQC spectra indicated 30 carbons (Table 3) comprising 11 quaternary carbons (δ_C 205.4, 171.0, 164.8, 161.5, 149.2, 148.8, 124.0, 105.9, 79.0, 45.9, 36.9), 3 methine carbons (δ_C 121.5, 52.5, 45.6), 11 methylene carbons (δ_C 107.6, 106.8, 54.5, 41.3, 36.2, 36.2, 32.7, 26.0, 25.4, 23.0, 22.4) and 5 methyl carbons (δ_C 29.7, 26.0, 16.9, 15.5, 8.4). These spectral characteristics closely resembled those of atractylenolide III and (5*S*,10*S*)-eudesm-4(15),7-diene-11-ol-9-one [17], except for the chemical shift deviations at C-8 in atractylenolide III and C-11 in **17**. These differences suggest that **16** may be an adductive derivative resulting from a structural fusion or modification of these two scaffolds. The planar structure of **16** was established through analysis of HMBC and ^{1}H–^{1}H COSY correlations (Fig. 2). The atractylenolide III fragment was confirmed by HMBCs between H-13′ (δ_H 1.78) and C-7′ (δ_C 161.5), C-11′ (δ_C 124.0), C-12′ (δ_C 171.0), between H-14′ (δ_H 1.00) and C-1′ (δ_C 41.3), C-5′ (δ_C 52.5), C-9′ (δ_C 54.5), C-10′ (δ_C 36.9), between H-15′ (δ_H 4.86, 4.59) and C-3′ (δ_C 36.2), C-4′ (δ_C 148.8), C-5′ (δ_C 52.5) and the ^{1}H–^{1}H COSY correlations of H-1′–H-2′–H-3′. The (5*S*,10*S*)-eudesm-4(15),7-diene-11-ol-9-one motif was established through HMBCs from H-8 (δ_H 5.68) to C-6 (δ_C 25.4), C-7 (δ_C 164.8), C-9 (δ_C 205.4), C-11 (δ_C 79.0), from H-12, H-13 to C-7, C-11, from H-14 (δ_H 0.88) to C-1 (δ_C 32.7), C-5 (δ_C 45.6), C-9, C-10 (δ_C 45.9), from H-15 to C-3 (δ_C 36.2), C-4 (δ_C 149.2), C-5. The connection between atractylenolide III and (5*S*,10*S*)-eudesm-4(15),7-diene-11-ol-9-one *via* C_{11}-O-$C_{8'}$ was determined by their chemical shifts (δ_C 79.0 for C-11 and 105.9 for C-8′). Biogenetically, H-5 and H-5′ were assigned as *α*-oriented, while 14-Me and 14′-Me were assigned as *β*-oriented. C-8′ was established as the *S* configuration based on the chemical shifts of C-5′ (δ_C 52.5) and C-10′ (δ_C 36.9). The absolute configuration of **16** was confirmed as 5*S*,10*S*,5′*S*,8′*S*,10′*R* through comparison of experimental and calculated CD curves (Fig. S1).

The isolates, excluding compounds **8** and **15**, were evaluated for cytotoxic activities against HepG2, Hep3B, and Huh7 cell lines. As indicated in Table 4, compounds **1**, **4**–**7**, **9**, and **10** demonstrated significant cytotoxicity against HepG2 cells with half maximal inhibitory concentration (IC_{50}) values of 8.47, 11.30, 6.34, 5.78, 9.85, 12.51, and 7.79 μmol·L^{-1}, comparable to sorafenib (IC_{50} 9.48 μmol·L^{-1}). Compounds **2**, **11**, **13**, **14**, **16**–**18** exhibited moderate cytotoxicity with IC_{50} values ranging from 15.98 to 29.63 μmol·L^{-1}. Against Hep3B cells, compounds **1**, **2**, **4**–**7**, **9**–**11**, **13**, **14**, **16**–**18** showed moderate cytotoxicity with IC_{50} values ranging from 5.42 to 22.34 μmol·L^{-1} (sorafenib IC_{50} 3.19 μmol·L^{-1}). For Huh7 cells, compounds **1**, **4**–**7**, **9**, **10**, and **13** exhibited notable cytotoxicity with IC_{50} values of 4.30, 8.12, 8.99, 3.71, 7.29, 13.99, 10.21, and 8.63 μmol·L^{-1}, similar to sorafenib (IC_{50} 9.53 μmol·L^{-1}). Compounds **2**, **3**, **11**, **14**, and **16**–**18** demonstrated moderate cytotoxicity with IC_{50} values ranging from 17.41 to 23.01 μmol·L^{-1}.

3. Conclusions

Thirteen distinctive rearranged 9(8→7)-*abeo*-eudesmane-

Table 4 Cytotoxic activities of compounds **1**–**7**, **9**–**14**, and **16**–**18** against Hep3B, HepG2, and Huh7 cells [IC_{50}/(μmol·L^{-1}); mean ± SD, *n* = 3].

Compounds	HepG2	Hep3B	Huh-7
1	8.47 ± 0.66	9.18 ± 0.11	4.30 ± 0.19
2	15.98 ± 0.44	9.34 ± 0.60	17.41 ± 0.64
3	> 40	> 40	22.85 ± 1.88
4	11.30 ± 0.12	8.81 ± 0.29	8.12 ± 0.21
5	6.34 ± 0.62	7.33 ± 0.67	8.99 ± 0.04
6	5.78 ± 0.42	8.89 ± 0.44	3.71 ± 0.02
7	9.85 ± 0.17	6.11 ± 0.40	7.29 ± 0.38
9	12.51 ± 0.45	9.73 ± 0.43	13.99 ± 0.46
10	7.79 ± 1.26	5.42 ± 0.32	10.21 ± 0.70
11	26.86 ± 0.41	18.88 ± 0.21	21.43 ± 0.07
12	> 40	> 40	> 40
13	18.27 ± 0.98	11.15 ± 1.22	8.63 ± 0.27
14	17.94 ± 0.10	16.59 ± 0.53	17.00 ± 0.32
16	27.90 ± 1.39	20.83 ± 0.07	22.08 ± 0.45
17	29.63 ± 0.35	19.60 ± 0.19	20.46 ± 0.61
18	26.96 ± 0.17	22.34 ± 0.56	23.01 ± 0.92
Sorafenib	9.48 ± 0.50	3.19 ± 0.39	9.53 ± 0.23

type SDs, atramacronins A–M (**1**–**13**), three eudesmane-type SDs, atramacronins N–P (**14**–**16**), along with one known meroterpenoid, atrachinenin G (**8**), were isolated from *A. macrocephala*. Compounds **1**–**11** exhibited identical planar structures with varying absolute configurations in the newly formed five-membered lactone ring. The rare spiro skeleton in compounds **1**–**11** likely originated from eudesmanolide *via* a pinacol rearrangement, similar to that of ligulactone A and B [18]. Compound **12** represented a rare rearranged norsesquiterpenoid dimer. Compounds **1**, **4**–**7**, **9**, and **10** demonstrated significant cytotoxic activities against three liver cancer cell lines (Hep3B, HepG2, and Huh7) with IC_{50} values ranging from 3.71 to 13.99 μmol·L^{-1}. These findings enhance understanding of the chemical composition of *A. macrocephala* and identify several potent SDs effective against HCC.

4. Experimental

4.1. General experimental procedures

Normal phase silica gel (100–200 and 200–300 mesh) for column chromatography (CC) was obtained from Qingdao Marine Chemical Factory (Qingdao, China). Sephadex LH-20 was provided by GE Healthcare Life Sciences China (Beijing, China). ODS-A-HG (12 nm, S-50 μm) for medium-pressure liquid chromatography was acquired from YMC Co., Ltd. (Japan). Semipreparative high-performance liquid chromatography (HPLC) experiments were performed on a STI501 HPLC (Surwit Technology Inc., Hangzhou, China) equipped with a Cosmosil $5C_{18}$-MS-II column (250 mm × 10 mm, 5 μm, Nacalai Tesque, Inc., Kyoto, Japan) or a Cosmosil cholester column (250 mm × 10 mm, 5 μm, Nacalai Tesque, Inc., Kyoto, Japan). High-resolution mass spectra were recorded on a Thermo QE plus mass spectrometer (Thermo Electron, Bremen, Germany). UV spectra were measured on a Shimadzu UV-2550 spectrophotometer (Shimadzu Crop., Kyoto, Japan). IR spectra were obtained on a Shimadzu IRTracer-100 spectrophotometer with KBr pellets (Shimadzu Co., Japan). NMR spectra were obtained on a Bruker AV-400 spectrometer (Bruker, Bremen, German). Deuterated $CDCl_3$ was supplied by Ningbo Cuiying Chemical Technology Co., Ltd. (Ningbo, China). ORD was recorded on an Anton Paar MCP 5100 polarimeter (Anton Paar Co., Ltd., Graz, Austria). CD spectra were measured on a Chirascan VX spectrometer (Applied Photophysics Ltd., United Kingdom). Crystal structures were measured on a SuperNova, Dual, Cu at zero, Atlas S2 diffractometer (Agilent, American). Human liver cancer HepG2, Hep3B, and Huh7 cell lines were obtained from Wuhan Pricella Biotechnology Co., Ltd. (Wuhan, China). Cells were cultured in Biosharp® MEM-α medium (Labgic Technology Co., Ltd., Hefei, China) containing 10% fetal bovine serum (Cegrogen Biotech GmbH, Germany) and 1% penicillin/streptomycin in a 311 humidified incubator (Thermo Fisher Scientific Co., Ltd., Bremen, Germany) at 37 °C in an atmosphere of 5% CO_2.

4.2. Plant material

Dried rhizoma of *A. macrocephala* were collected from the Lotus Pond Chinese Herbal Medicine Market, Chengdu, Sichuan Province, in September 2022, and identified by Prof. Xiaozhong Lan (Xizang Agriculture and Animal Husbandry College). A voucher specimen (No. 2022-AM-1001) has been deposited at the College of Pharmaceutical Sciences, Southwest University, Chongqing, China.

4.3. Extraction and isolation

The dried rhizomes of *A. macrocephala* were pulverized and extracted with 95% ethanol overnight (10-fold *V*/*W*, three times), yielding an ethanol extract (4.43 kg). This extract was suspended in water and subsequently extracted with ethyl acetate (EtOAc) to obtain the EtOAc extract (1.80 kg). The EtOAc extract underwent fractionation *via* silica gel CC using petroleum ether–EtOAc (100∶0–0∶100) as the eluent, producing 7 fractions (Fr. A–G). Fraction C (337 g) was further separated on silica gel CC using petroleum ether–EtOAc (50∶1–0∶100) as the eluent, resulting in 22 subfractions (Fr. C1–C22).

Fraction C14 (25.2 g) underwent separation on a medium-pressure ODS CC (1300 mL ODS, CH_3OH∶H_2O, 50∶50 to 100∶0), yielding 22 subfractions, Fr. C14-1–C14-22. Fr. C14-12 (348 mg) was subjected to silica gel CC with petroleum ether–EtOAc from 10∶1 to 0∶1 to produce 5 subfractions (Fr. C14-12-1–C14-12-5). Compound **3** (67.2 mg) was isolated from Fr. C14-12-2 *via* recrystallization. The mother liquor (144 mg) underwent purification by semi-preparative HPLC (Cosmosil cholester 10 mm × 250 mm, CH_3CN∶H_2O, 63∶37, 3 mL·min^{-1}) to afford compound **8** (2.3 mg, t_R 28.81 min). Fr. C14-13 (1.34 g) was fractionated on silica gel CC using a gradient eluent of petroleum ether–EtOAc from 10∶1 to 0∶1, resulting in 6 subfractions (Fr. C14-13-1–C14-13-6). Fr. C14-13-4 (859 mg) underwent separation on medium-pressure ODS CC (200 mL ODS, CH_3OH∶H_2O, 80∶20 to 100∶0) to generate 6 subfractions (Fr. C14-13-4-1–C14-13-4-6). Fr. C14-13-4-3 (480 mg) was purified through semi-preparative HPLC (Cosmosil $5C_{18}$-MS-II 10 mm × 250 mm, CH_3OH∶H_2O, 88∶12, 3 mL·min^{-1}), yielding compounds **17** (90.5 mg, t_R 33.60 min), **2** (57.4 mg, t_R 35.86 min) and a mixture. The mixture underwent further separation by semi-preparative HPLC (Cosmosil cholester 10 mm × 250 mm, CH_3OH∶H_2O, 85∶15, 2 mL·min^{-1}) to yield compounds **11** (12.2 mg, t_R 50.11 min) and **7** (3.4 mg, t_R 52.62 min). Fr. C14-13-4-4 (173 mg) was purified *via* semi-preparative HPLC (Cosmosil $5C_{18}$-MS-II 10 mm × 250 mm, CH_3OH∶H_2O, 91∶9, 3 mL·min^{-1}, then Cosmosil cholester 10 mm × 250 mm, CH_3CN∶H_2O, 80∶20, 3 mL·min^{-1}) to obtain compound **18** (30.1 mg, t_R 38.72 min). Fr. C14-15 (1.077g) underwent fractionation on silica gel column (petroleum ether–EtOAc, 100∶0–0∶100), yielding Fr. C14-15-1–Fr. C14-15-6. Fr. C14-15-2 (551 mg) was purified through semi-preparative HPLC (Cosmosil cholester 10 mm × 250 mm, CH_3CN∶H_2O, 92∶8, 2 mL·min^{-1}) to afford compounds **16** (11.5 mg, t_R 28.47 min) and a mixture. The mixture underwent further separation by semi-preparative HPLC (Cosmosil $5C_{18}$-MS-II 10 mm × 250 mm, CH_3CN∶H_2O, 90∶10, 2 mL·min^{-1}) to yield compounds **14** (12.1 mg, t_R 35.03 min) and **15** (2.4 mg, t_R 26.38 min).

Fraction C19 (29.7 g) underwent further separation on silica gel CC using petroleum ether–EtOAc (50∶1 to 0∶1) as eluent, yielding 11 subfractions (Fr. C19-1–C19-11). Fr. C19-4 (10.1 g) was subjected to medium-pressure ODS CC (400 mL ODS, CH_3OH∶H_2O, 60∶40 to 100∶0), producing 25 subfractions, Fr. C19-4-1–C19-4-25. Fr. C19-4-13 (127 mg) was purified *via* semi-preparative HPLC (Cosmosil $5C_{18}$-MS-II 10 mm × 250 mm, CH_3CN∶H_2O, 68∶32, 3 mL·min^{-1}) to obtain compound **12** (7.5 mg, t_R 30.47 min). Fr. C19-4-15 (238 mg) underwent semi-preparative HPLC (Cosmosil cholester 10 mm × 250 mm, CH_3CN∶H_2O, 68∶32, 3 mL·min^{-1}), yielding compounds **5** (45.8 mg, t_R 37.71 min) and **10** (24.8 mg, t_R 45.72 min). Fr. C19-4-18 (588 mg) was fractionated through a Sephadex LH-20 column with CH_3OH elution to produce Fr. C19-4-18-1–Fr. C19-4-18-4. Fr. C19-4-18-3 (299 mg) underwent semi-preparative HPLC (Cosmosil $5C_{18}$-MS-II 10 mm × 250 mm, CH_3OH∶H_2O, 85∶15, 3 mL·min^{-1}, followed by Cosmosil cholester 10 mm × 250 mm, CH_3CN∶H_2O, 73∶27, 3 mL·min^{-1}), yielding compound **9** (47.0 mg, t_R 52.15 min). Fr. C19-5 (7.6 g) was purified through medium-pressure ODS CC (400 mL ODS, CH_3OH∶H_2O, 60∶40 to 100∶0), generating 16 subfractions, Fr. C19-5-1–C19-5-16. Fr. C19-5-12 (488 mg) underwent semi-preparative HPLC (Cosmosil $5C_{18}$-MS-II 10 mm × 250 mm, CH_3OH∶H_2O, 80∶20), producing three fractions, Fr. C19-5-12-

1–Fr. C19-5-12-3. Fr. C19-5-12-1 was purified *via* semi-preparative HPLC (Cosmosil 5C_{18}-MS-II 10 mm × 250 mm, CH_3CN∶H_2O, 71∶29, 3 mL·min^{-1}), yielding compound **4** (51.1 mg, t_R 32.75 min). Compound **6** (13.3 mg, t_R 32.60 min) was isolated from Fr. C19-5-12-2 through semi-preparative HPLC (Cosmosil 5C_{18}-MS-II 10 mm × 250 mm, CH_3CN∶H_2O, 72∶28, 3 mL·min^{-1}). Fr. C19-5-12-3 underwent additional semi-preparative HPLC (Cosmosil 5C_{18}-MS-II 10 mm × 250 mm, CH_3CN∶H_2O, 71∶29, 3 mL·min^{-1}), yielding compound **1** (210.4 mg, t_R 33.57 min).

Fr. C22 (18.2 g) was fractionated by silica gel CC (petroleum ether–EtOAc, 10∶1–0∶1), yielding Fr. C22-1–Fr. C22-14. Fr. C22-8 (4.5 g) underwent further separation *via* MPLC (400 mL ODS, 50%–100% CH_3OH, 15 mL·min^{-1}) to produce Fr. C22-8-1–Fr. C22-8-22. Compound **13** (4.1 mg, t_R 27.54 min) was isolated from Fr. C22-8-12 using semi-preparative HPLC (Cosmosil cholester 10 mm × 250 mm, CH_3CN∶H_2O, 63∶37, 3 mL·min^{-1}).

Atramacronin A (**1**): colorless bulk crystal, $[\alpha]_D^{25}$ +200.9 (*c* 0.33, CH_3OH); UV (CH_3OH) λ_{max} (log ε) 218 (4.13), CD (MeOH) λ ($\Delta\varepsilon$) 240 (+18.60) nm; IR (KBr) cm^{-1}: 3445, 2974, 2945, 2841, 1749, 1697, 1647, 1443, 1389, 1323, 989, 943, 881; HR-ESI-MS *m/z* 519.2711 (Calcd. for $C_{30}H_{40}O_6Na^+$, 519.2718); ^{1}H and ^{13}C NMR data see in Table 1. X-ray crystal data: $C_{30}H_{40}O_6$, *M* = 496.62 g·mol^{-1}, orthorhombic, space group $P2_12_12_1$, *a* = 11.8256 (4) Å, *b* = 13.4429 (4) Å, *c* = 17.0216 (5) Å, α = 90, β = 90, γ = 90, *V* = 2705.93 (15) Å^3, *Z* = 4, μ(Cu Kα) = 0.672 mm^{-1}, ρ_{calc} = 1.219 g·cm^{-3}, F(000) = 1072.0; crystal size: 0.24 × 0.22 × 0.2 mm^3; 12 727 reflections measured (4.191° ≤ 2Θ ≤ 65.080°), 4454 unique (R_{int} = 0.0748), final R_1 = 0.0622 [I > 2σ(I)], wR_2 = 0.1646 (all data), flack parameter = 0.0 (3); supplementary publication No. CCDC-2351821.

Atramacronin B (**2**): colorless bulk crystal, $[\alpha]_D^{25}$ +76.6 (*c* 0.28, CH_3OH); UV (CH_3OH) λ_{max} (log ε) 219 (4.20), CD (MeOH) λ ($\Delta\varepsilon$) 205 (+57.44), 300 (+32.54) nm; IR (KBr) cm^{-1}: 3446, 2976, 2934, 2870, 1774, 1689, 1649, 1453, 1445, 1323, 1151, 1119, 991, 941, 889; HR-ESI-MS *m/z* 519.2712 (Calcd. for $C_{30}H_{40}O_6Na^+$, 519.2718); ^{1}H and ^{13}C NMR data see in Table 1. X-ray crystal data: $C_{30}H_{40}O_6$, *M* = 496.62 g·mol^{-1}, orthorhombic, space group $P2_12_12$, *a* = 9.390 30 (18) Å, *b* = 19.2391 (4) Å, *c* = 18.2149 (4) Å, α = 90, β = 90, γ = 90, *V* = 3290.72 (12) Å^3, *Z* = 4, *T* = 169.99 (10) K, μ (Cu Kα) = 0.553 mm^{-1}, ρ_{calc} = 1.002 g·cm^{-3}, F(000) = 1072.0; crystal size: 0.16 × 0.12 × 0.09 mm^3; 22 485 reflections measured (4.852° ≤ 2Θ ≤ 133.17°), 5831 unique (R_{int} = 0.0525, R_{sigma} = 0.0391), final R_1 = 0.0412 [I > 2σ(I)], wR_2 = 0.1045 (all data), flack parameter = 0.08 (11); supplementary publication No. CCDC-2351822.

Atramacronin C (**3**): colorless bulk crystal, $[\alpha]_D^{25}$ +66.4 (*c* 0.23, CH_3OH); UV (CH_3OH) λ_{max} (log ε) 219 (4.11), CD (MeOH) λ ($\Delta\varepsilon$) 210 (+1.59), 245 (+15.61) nm; IR (KBr) cm^{-1}: 3487, 3452, 2987, 2928, 2849, 1769, 1691, 1649, 1441, 1385, 1319, 1109, 997, 931; HR-ESI-MS *m/z* 519.2711 (Calcd. for $C_{30}H_{40}O_6Na^+$, 519.2718); ^{1}H and ^{13}C NMR data see in Table 1. X-ray crystal data: $C_{30}H_{40}O_6$, *M* = 496.62 g·mol^{-1}, orthorhombic, space group $P2_12_12_1$, *a* = 12.534 26 (15) Å, *b* = 12.886 47 (15) Å, *c* = 16.981 51 (19) Å, α = 90, β = 90, γ = 90, *V* = 2742.89 (6) Å^3, *Z* = 4, *T* = 150.00 (10) K, μ(Cu Kα) = 0.663 mm^{-1}, ρ_{calc} = 1.203 g·cm^{-3}, F(000) = 1072.0; crystal size: 0.16 × 0.14 × 0.12 mm^3; 10 825 reflections measured (8.614° ≤ 2Θ ≤ 147.524°), 5319 unique (R_{int} = 0.0291, R_{sigma} = 0.0339), final R_1 = 0.0382 [I > 2σ(I)], wR_2 = 0.1031 (all data), flack parameter = −0.03 (8); supplementary publication No. CCDC-2351823.

Atramacronin D (**4**): white amorphous powder, $[\alpha]_D^{25}$ +127.9 (*c* 0.55, CH_3OH); UV (CH_3OH) λ_{max} (log ε) 219 (4.00), CD (MeOH) λ ($\Delta\varepsilon$) 239 (+7.48) nm; IR (KBr) cm^{-1}: 3449, 2976, 2932, 2864, 1778, 1689, 1649, 1450, 1381, 1319, 1284, 1149, 1089, 898, 941, 885; HR-ESI-MS *m/z* 519.2708 (Calcd. for $C_{30}H_{40}O_6Na^+$, 519.2718); ^{1}H and ^{13}C NMR data see in Table 1. X-ray crystal data: $C_{30}H_{40}O_6$, *M* = 496.62 g·mol^{-1}, monoclinic, space group $P2_1$, *a* = 10.5505 (2) Å, *b* = 23.0161 (5) Å, *c* = 11.1928 (2) Å, α = 90, β = 91.617 (2), γ = 90, *V* = 2716.88 (9) Å^3, *Z* = 4, *T* = 169.99 (10) K, μ(Cu Kα) = 0.669 mm^{-1}, ρ_{calc} = 1.214 g·cm^{-3}, F(000) = 1072.0; crystal size: 0.15 × 0.12 × 0.11 mm^3; 27 704 reflections measured (7.682° ≤ 2Θ ≤ 147.836°), 10 678 unique (R_{int} = 0.0416, R_{sigma} = 0.0436), final R_1 = 0.0507 [I > 2σ(I)], wR_2 = 0.1424 (all data), flack parameter = −0.09 (10); supplementary publication No. CCDC-2351825.

Atramacronin E (**5**): white amorphous powder, $[\alpha]_D^{25}$ +94.4 (*c* 0.11, CH_3OH); UV (CH_3OH) λ_{max} (log ε) 219 (4.00), CD (MeOH) λ ($\Delta\varepsilon$) 205 (−0.85), 218 (+0.28), 246 (+4.45) nm; IR (KBr) cm^{-1}: 3524, 2972, 2932, 2856, 1776, 1689, 1647, 1443, 1381, 1319, 1092, 991, 956, 931, 887; HR-ESI-MS *m/z* 519.2712 (Calcd. for $C_{30}H_{40}O_6Na^+$, 519.2718); ^{1}H and ^{13}C NMR data see in Table 1.

Atramacronin F (**6**): white amorphous powder, $[\alpha]_D^{25}$ +6.4 (*c* 0.13, CH_3OH); UV (CH_3OH) λ_{max} (log ε) 217 (4.06), CD (MeOH) λ ($\Delta\varepsilon$) 208 (−2.65), 222 (+1.16), 245 (−5.15) nm; IR (KBr) cm^{-1}: 3505, 3445, 3383, 2930, 2862, 1776, 1695, 1651, 1443, 1387, 1327, 1234, 1147, 1094, 960, 893; HR-ESI-MS *m/z* 519.2712 (Calcd. for $C_{30}H_{40}O_6Na^+$, 519.2718); ^{1}H and ^{13}C NMR data see in Table 1.

Atramacronin G (**7**): white amorphous powder, $[\alpha]_D^{25}$ +34.5 (*c* 0.42, CH_3OH); UV (CH_3OH) λ_{max} (log ε) 216 (4.09), CD (MeOH) λ ($\Delta\varepsilon$) 202 (−18.38), 223 (+9.30), 246 (−10.40) nm; IR (KBr) cm^{-1}: 3462, 3419, 2934, 2849, 1769, 1642, 1437, 1381, 1331, 1254, 1126, 1099, 941, 891; HR-ESI-MS *m/z* 519.2708 (Calcd. for $C_{30}H_{40}O_6Na^+$, 519.2718); ^{1}H and ^{13}C NMR data see in Table 2.

Atramacronin H (**8**): white amorphous powder, $[\alpha]_D^{25}$ +61.4 (*c* 0.50, CH_3OH); UV (CH_3OH) λ_{max} (log ε) 218 (4.04), CD (MeOH) λ ($\Delta\varepsilon$) 201 (−27.73), 222 (+6.60), 245 (−10.04) nm; IR (KBr) cm^{-1}: 3433, 2932, 2856, 1773, 1643, 1452, 1383, 1259, 1115, 953, 889; HR-ESI-MS *m/z* 519.2706 (Calcd. for $C_{30}H_{40}O_6Na^+$, 519.2718); ^{1}H and ^{13}C NMR data see in Table 2.

Atramacronin I (**9**): white amorphous powder, $[\alpha]_D^{25}$ +64.6 (*c* 0.13, CH_3OH); UV (CH_3OH) λ_{max} (log ε) 218 (4.08), CD (MeOH) λ ($\Delta\varepsilon$) 206 (+6.64), 238 (+11.33) nm; IR (KBr) cm^{-1}: 3456, 2932, 2847, 1769, 1645, 1448, 1387, 1319, 1149, 1088, 930, 889; HR-ESI-MS *m/z* 519.2707 (Calcd. for $C_{30}H_{40}O_6Na^+$, 519.2718); ^{1}H and ^{13}C NMR data see in Table 2.

Atramacronin J (**10**): white amorphous powder, $[\alpha]_D^{25}$ −15.0 (*c* 0.18, CH_3OH); UV (CH_3OH) λ_{max} (log ε) 219 (4.07), CD (MeOH) λ ($\Delta\varepsilon$) 241 (+10.68) nm; IR (KBr) cm^{-1}: 3446, 3391, 2932, 2870, 1775, 1647, 1446, 1387, 1327, 1151, 1118, 951, 893; HR-ESI-MS *m/z* 519.2709 (Calcd. for $C_{30}H_{40}O_6Na^+$, 519.2718); ^{1}H and ^{13}C NMR data see in Table 2.

Atramacronin K (**11**): white amorphous powder, $[\alpha]_D^{25}$ +113.7 (*c* 0.15, CH_3OH); UV (CH_3OH) λ_{max} (log ε) 217 (4.06), CD (MeOH) λ ($\Delta\varepsilon$) 201 (−48.13), 224 (+9.21), 246 (−16.63) nm; IR (KBr) cm^{-1}: 3435, 3348, 2934, 2868, 2843, 1745, 1656, 1589, 1445, 1379, 1325, 1196, 1127, 962, 951, 885; HR-ESI-MS *m/z* 519.2711 (Calcd. for $C_{30}H_{40}O_6Na^+$, 519.2718); ^{1}H and ^{13}C NMR data see in Table 2.

Atramacronin L (**12**): white amorphous powder, $[\alpha]_D^{25}$ −15.0 (*c* 0.03, CH_3OH); CD (MeOH) λ ($\Delta\varepsilon$) 207 (−9.26) nm; IR (KBr) cm^{-1}: 3506, 3445, 3387, 2934, 2862, 1718, 1645, 1603, 1381, 1325, 1288, 1194, 1147, 1120, 1095, 1002, 958, 933, 887; HR-ESI-MS *m/z* 451.2813 (Calcd. for $C_{27}H_{40}O_4Na^+$, 451.2819); ^{1}H and ^{13}C NMR data see in Table 3.

Atramacronin M (**13**): white amorphous powder, $[\alpha]_D^{25}$ +95.2 (*c* 0.30, CH_3OH); CD (MeOH) λ ($\Delta\varepsilon$) 206 (+14.72) nm; IR (KBr) cm^{-1}: 3541, 3470, 3423, 2984, 2934, 2866, 1775, 1620, 1381, 1346, 1120, 989, 925; HR-ESI-MS *m/z* 521.2867 (Calcd. for $C_{30}H_{42}O_6Na^+$, 521.2874); ^{1}H and ^{13}C NMR data see in Table 3.

Atramacronin N (**14**): white amorphous powder, $[\alpha]_D^{25}$ +104.1 (*c* 0.48, CH_3OH); UV (CH_3OH) λ_{max} (log ε) 218 (3.18), CD (MeOH) λ ($\Delta\varepsilon$) 224 (+24.75) nm; IR (KBr) cm^{-1}: 2934, 1763, 1695, 1645, 144, 1379, 1182, 1082, 947, 889; HR-ESI-MS *m/z* 489.2964 (Cal-

cd. for $C_{30}H_{42}O_4Na^+$, 489.2976); ^1H and ^{13}C NMR data see in Table 3.

Atramacronin O (**15**): white amorphous powder, $[\alpha]_D^{25}$ +71.6 (*c* 0.25, CH_3OH); UV (CH_3OH) λ_{max} (log ε) 218 (3.20), CD (MeOH) λ ($\Delta\varepsilon$) 231 (+27.74) nm; IR (KBr) cm^{-1}: 3587, 3518, 3449, 2935, 1763, 1693, 1599, 1441, 1390, 1313, 1178, 1080, 945, 885; HR-ESI-MS *m/z* 489.2963 (Calcd. for $C_{30}H_{42}O_4Na^+$, 489.2976); ^1H and ^{13}C NMR data see in Table 3.

Atramacronin P (**16**): white amorphous powder, $[\alpha]_D^{25}$ +140.3 (*c* 0.83, CH_3OH); UV (CH_3OH) λ_{max} (log ε) 222 (2.93), CD (MeOH) λ ($\Delta\varepsilon$) 224 (+34.64), 248 (+10.17) nm; IR (KBr) cm^{-1}: 3420, 2934, 2864, 1763, 1668, 1441, 1381, 1138, 1115, 951, 887; HR-ESI-MS *m/z* 487.2805 (Calcd. for $C_{30}H_{40}O_4Na^+$, 487.2819); ^1H and ^{13}C NMR data see in Table 3.

Atrachinenin G (**17**) X-ray crystal data: $C_{32}H_{42}O_4$, M = 490.65 g·mol^{-1}, monoclinic, space group $P2_1$, a = 6.575 13 (10) Å, b = 17.3196 (3) Å, c = 12.4082 (2) Å, α = 90, β = 90.5553 (14), γ = 90, V = 1412.96 (4) Å^3, Z = 2, T = 150.00 (10) K, μ(Cu Kα) = 0.583 mm^{-1}, ρ_{calc} = 1.153 g·cm^{-3}, F(000) = 532.0; crystal size: 0.14 × 0.12 × 0.09 mm^3; 12 419 reflections measured (7.124° ≤ 2Θ ≤ 147.324°), 4930 unique (R_{int} = 0.0580, R_{sigma} = 0.0470), final R_1 = 0.0545 [I > 2σ(I)], wR_2 = 0.1498 (all data), flack parameter = −0.36 (19); supplementary publication No. CCDC-2351824.

4.4. Quantum chemical calculation

Based on the NMR data, plausible enantiomers of each compound were selected for calculation. Systematic random conformational analyses were conducted using MMFF94s molecular force field, with an energy cutoff of 10 kcal·mol^{-1} relative to global minima. All conformers were subsequently optimized using DFT at the B3LYP/6-31 + G(d) level in the gas phase utilizing Gaussian09 software [19]. The optimized stable conformers were employed for TDDFT computation at the same calculation level, considering the first 180 excitations. The overall electronic circular dichroism (ECD) curves were weighted by Boltzmann distribution. ECD spectra were generated using SpecDis 1.70.1 software. For NMR calculations, all conformers were optimized using DFT at the B3LYP/6-31G(d) level in the gas phase and computed at the same calculation level with chloroform as solvent. The overall chemical shifts were weighted by Boltzmann distribution and scaled using computed NMR scaling factors [20].

4.5. Cell viability assay

The cytotoxic activities of compounds **1**–**7**, **9**–**14**, and **16**–**18** were evaluated using the methyl thiazolyl tetrazolium (MTT) method on HepG2, Hep3B, and Huh7 cell lines. Cells were seeded into 96-well plates (1 × 10^4 cells/well) and incubated for 24 h. The medium was replaced with fresh medium containing various concentrations of compounds (0–40 μmol·L^{-1}), and cells were incubated for an additional 48 h. Subsequently, the medium was removed and 20 μL of MTT reagent (1 mg·mL^{-1}) was added to each well. Following 4 h incubation, 100 μL of DMSO was added to each well, and absorbance at 490 nm was measured using a Bio-Tek Synergy H1 microplate reader (Gene Company Limited, Hong Kong, China). The inhibitory ratio was calculated as $[(A_{control} - A_{compound})/A_{control}] \times 100\%$. IC_{50} values were calculated using GraphPad Prism 9.5 (GraphPad Software, California, USA).

Funding

This work was supported by the National Natural Science Foundation of China (Nos. 32470414, 32100319, and 82104377), the Fundamental Research Funds for the Central Universities, SWU (No. SWU-KR22052), the Natural Science Foundation of Chongqing, China (No. CSTB2022NSCQMSX0878) and Chongqing Municipal Training Program of Innovation and Entrepreneurship for Undergraduates (No. S20241063290).

Supporting information

The Supporting information for 1D and 2D NMR, HR-ESI-MS, UV and IR spectra, and calculating details of compounds **1**–**16** can be requested by sending E-mails to the corresponding authors.

Declaration of competing interest

These authors have no conflict of interest to declare.

References

1 Yang L, Yu H, Hou A, et al. A review of the ethnopharmacology, phytochemistry, pharmacology, application, quality control, processing, toxicology, and pharmacokinetics of the dried rhizome of *Atractylodes macrocephala*. *Front Pharmacol*. 2021;12:727154. https://doi.org/10.3389/fphar.2021.727154.
2 Pei T, Dai Y, Tan X, et al. Yupingfeng San exhibits anticancer effect in hepatocellular carcinoma cells *via* the MAPK pathway revealed by HTS^2 technology. *J Ethnopharmacol*. 2023;306:116134. https://doi.org/10.1016/j.jep.2023.116134.
3 Yang X, Feng Y, Liu Y, et al. Fuzheng Jiedu Xiaoji Formulation inhibits hepatocellular carcinoma progression in patients by targeting the AKT/CyclinD1/p21/p27 pathway. *Phytomedicine*. 2021;87:153575. https://doi.org/10.1016/j.phymed.2021.153575.
4 Bailly C. Atractylenolides, essential components of atractylodes-based traditional herbal medicines: antioxidant, anti-inflammatory and anticancer properties. *Eur J Pharmacol*. 2021;891:173735. https://doi.org/10.1016/j.ejphar.2020.173735.
5 Jiang Y, Guo K, Wang P, et al. The antitumor properties of atractylenolides: molecular mechanisms and signaling pathways. *Biomed Pharmacother*. 2022;155:113699. https://doi.org/10.1016/j.biopha.2022.113699.
6 Ma L, Chen Y, Shan W, et al. Natural disesquiterpenoids: an update. *Nat Prod Rep*. 2020;37:999-1030. https://doi.org/10.1039/C9NP00062C.
7 Ma Y, Dou X, Tian X. Natural disesquiterpenoids: an overview of their chemical structures, pharmacological activities, and biosynthetic pathways. *Phytochem Rev*. 2020;19:983-1043. https://doi.org/10.1007/s11101-020-09698-1.
8 Meng F, Wang Z, Peng S, et al. Recent advances of sesquiterpenoid dimers from Compositae: distribution, chemistry and biological activities. *Phytochem Rev*. 2024;23:625-655. https://doi.org/10.1007/s11101-023-09911-x.
9 Zhan ZJ, Ying YM, Ma LF, et al. Natural disesquiterpenoids. *Nat Prod Rep*. 2011;28:594-629. https://doi.org/10.1039/c0np00050g.
10 Zhao WY, Yan JJ, Liu TT, et al. Natural sesquiterpenoid oligomers: a chemical perspective. *Eur J Med Chem*. 2020;203:112622. https://doi.org/10.1016/j.ejmech.2020.112622.
11 Zhang H, Li J, Si J, et al. Atramacronoids A–C, three eudesmanolide sesquiterpene-phenol hybrids with an unprece dente d C-C linkage from the rhizomes of *Atractylodes macrocephala*. *Chin Chem Lett*. 2023;34:107743. https://doi.org/10.1016/j.cclet.2022.107743.
12 Chen F, Liu D, Fu J, et al. (±)-Atrachinenins A–C, three pairs of caged C27 meroterpenoids from the rhizomes of *Atractylodes chinensis*. *Chin J Chem*. 2021;40:460-466. https://doi.org/10.1002/cjoc.202100700.
13 Chen F, Liu D, Ren W, et al. Atrachinenins D–S, novel meroterpenoids with geranyl hydroquinone moiety from *Atractylodes chinensis* by the LC/MS-based molecular decoy and targeted isolation. *Bioorg Chem*. 2024;144:107111. https://doi.org/10.1016/j.bioorg.2024.107111.
14 Lauro G, Das P, Riccio R, et al. DFT/NMR approach for the configuration assignment of groups of stereoisomers by the combination and comparison of experimental and predicted sets of data. *J Org Chem*. 2020;85:3297-3306. https://doi.org/10.1021/acs.joc.9b03129.
15 Zhou Y, Gao H, Wu X, et al. Chemical constituents of petroleum ether extracted from *Atractylodes japonica*. *Acta Chin Med Pharm*. 2020;48(4):26-29. https://doi.org/10.19664/j.cnki.1002-2392.200209.
16 Zhao YN, Gao G, Ma JL, et al. Two new sesquiterpenes from the rhizomes of *Atractylodes macrocephala* and their biological activities. *Nat Prod Res*. 2022;36(5):1230-1235. https://doi.org/10.1080/14786419.2020.1869970.
17 Wang HX, Liu CM, Liu Q, et al. Three types of sesquiterpenes from rhizomes of *Atractylodes lancea*. *Phytochemistry*. 2008;69:2088-2094. https://doi.org/10.1016/j.phytochem.2008.04.008.
18 Zhang WJ, Li XH, Shi YP. A pair of epimeric spirosesquiterpenes from the roots of *Ligularia fischeri*. *J Nat Prod*. 2010;73:143-146. https://doi.org/10.1021/np900492b.
19 Meng FC, Ma YX, Zhan HH, et al. Lignans from the seeds of *Herpetospermum pedunculosum* and their farnesoid X receptor-activating effect. *Phytochemistry*. 2022;193:113010. https://doi.org/10.1016/j.phytochem.2021.113010.
20 Lodewyk MW, Soldi C, Jones PB, et al. The correct structure of aquatolide-experimental validation of a theoretically-predicted structural revision. *J Am Chem Soc*. 2012;134:18550-18553. https://doi.org/10.1021/ja3089394.